

Preferential Flow and Transport of *Cryptosporidium parvum* Oocysts through the Vadose Zone: Experiments and Modeling

Christophe J. G. Darnault, Tammo S. Steenhuis,* Patricia Garnier, Young-Jin Kim, Michael B. Jenkins, William C. Ghiorse, Philippe C. Baveye, and J.-Yves Parlange

ABSTRACT

As a result of *Cryptosporidium parvum* in drinking water, several outbreaks of cryptosporidiosis have occurred in the last 10 yr. Although it is generally believed that movement of pathogens through the soil is minimal, recent research has shown that appreciable numbers of *C. parvum* oocysts may be transported via preferential or fingered flow to groundwater. The objective of the present research was to further investigate and model the transport of oocysts through preferential flow paths in the vadose zone under a "worst-case" scenario. This was studied by adding calves feces containing *C. parvum* oocysts with a Cl^- tracer to undisturbed silt loam columns and disturbed sand columns during a simulated steady-state rain. The sand columns exhibited preferential flow in the form of fingers whereas macropore flow occurred in the undisturbed cores. In the columns with fingered flow, oocysts and Cl^- were transported rapidly with the same velocity through the columns. Although only 14 to 86% of the amount applied, the number of oocysts transported across the columns was several orders of magnitude above an infective dose. The macropore columns had only a very limited breakthrough of oocysts, which appeared several pore volumes after the Cl^- broke through initially. A simulation model for the transport of oocysts via preferential flow was developed on the basis of an existing preferential flow model for nonadsorbing solutes, with addition of a first-order sink term for adsorbance of the *C. parvum* to the air–water–solid (AWS) interfaces, and with velocity and dispersivity parameters derived from Cl^- transport. The breakthrough of *C. parvum* oocysts could be described realistically for the sand columns. However, the model could not describe oocyst transport in the columns with macropores.

PATHOGENIC BACTERIA, viruses, and protozoa in drinking water are a significant cause of animal and human death in many parts of the world. Chlorination is an efficient treatment against a wide range of pathogens, but is ineffective against several microorganisms, including the protozoan *Cryptosporidium parvum* (*C. parvum*), which causes cryptosporidiosis, a common waterborne disease (Smith et al., 1988; Smith, 1992; Craun et al., 1998). Although the active part of the *C. parvum* cycle occurs in the lower intestines of humans and domestic and wild animals, it is also present in the environment

in the form of 4- to 6- μm -long ovoid-shaped oocysts, with a double wall that is resistant to most oxidation processes such as ozonation and chlorination (Current, 1986; Atwill et al., 1997).

During the past two decades, the presence of *C. parvum* in surface- and groundwaters in the United States and Great Britain (Galbraith et al., 1987; Rose et al., 1991; Craun et al., 1998) has been associated with several major outbreaks of cryptosporidiosis (Hayes et al., 1989; MacKenzie et al., 1994). Among the different pathways for the transport of oocysts to drinking water sources, downward percolation is usually considered to be insignificant, because soils are generally assumed to be an effective filter for a wide range of pathogens. Studies of packed columns with saturated flow by Brush et al. (1999) and Harter et al. (2000) and undisturbed columns with unsaturated flow (Mawdsley et al., 1996), however, showed that *C. parvum* oocysts could be transported rapidly downward through the soil. Although transport of *C. parvum* oocysts in saturated flow has been studied experimentally and described mathematically (Brush et al., 1999; Harter et al., 2000), detailed observations of the transport and persistence of *C. parvum* oocysts in unsaturated soils with preferential flow are still lacking, particularly in the presence of preferential flow processes.

In this context, the overall objective of the present research was to investigate and model the transport of *C. parvum* oocysts through preferential flow paths in the vadose zone. Both fingered flow and macropore flow were investigated under simulated steady-state rainfall at rates much less than the saturated conductivity. The experiments represented a worst-case scenario where feces of calves containing *C. parvum* oocysts were applied during rainfall at the soil surface.

MATERIALS AND METHODS

Three sets of experiments were performed in which *C. parvum* oocysts contained in the feces of infected calves were placed on either homogeneous sand or undisturbed soil columns during simulated rainfall events. Different rain intensities (in one experimental set) together with the addition of a nonsorbing Cl^- tracer were used to better understand the role of preferential flow paths in the transport of *C. parvum* oocysts. FD&C blue dye #1 (also called brilliant blue) was used to visualize the flow paths.

In Exp. I and II, the columns consisted of 50 segments of Plexiglas tubing (14-cm i.d.), 1 cm high, held together by two large metal frames and secured by four hose clamps that were

C.J.G. Darnault, T.S. Steenhuis, Y.-J. Kim, and J.-Y. Parlange, Department of Biological and Environmental Engineering, Riley-Robb Hall, Cornell University, Ithaca, NY 14853; Patricia Garnier, INRA, Unité d'Agronomie de Laon-Peronne, 02007 Laon Cedex, France; M.B. Jenkins, USDA-ARS, Campbell Natural Resource Conservation Center, Watkinsville, GA 30677; W.C. Ghiorse, Department of Microbiology, Cornell University, Ithaca, NY 14853; P.C. Baveye, Laboratory of Geoenvironmental Engineering and Science, Department of Crop and Soil Sciences, Cornell University, Ithaca, NY 14853. Received 27 June 2003. Original Research Paper. *Corresponding author (tss1@cornell.edu).

Published in Vadose Zone Journal 3:262–270 (2004).
© Soil Science Society of America
677 S. Segoe Rd., Madison, WI 53711 USA

Abbreviations: AWS, air–water–solid; PBS, phosphate-buffered saline.

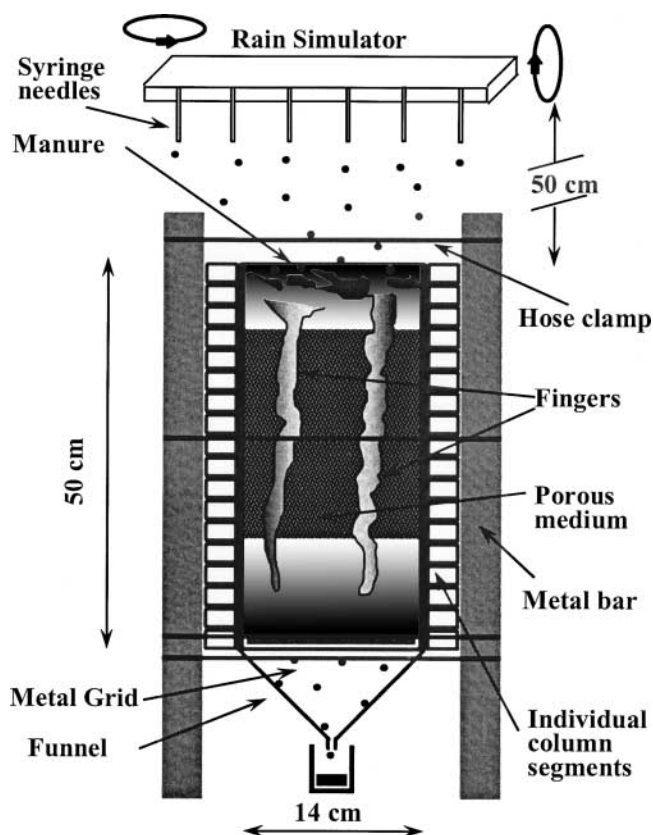


Fig. 1. Schematic illustration of the apparatus used in the laboratory experiments.

tightened to keep the rings in place (Fig. 1). At the bottom, the effluent flowed through a metal screen with a 0.5-mm mesh drop-through funnel into a sample container located immediately below. Sand was poured into the columns and packed to uniform density using a vibrator. In Exp. I, the columns contained industrial-quartz 12/20 silica sand (Union Corp.) with an average particle diameter of 1.1 mm. For Exp. II, the same 12/20 sand was used but made hydrophobic to different degrees by mixing in different portions of strongly water-repellent sand that was made by coating the regular 12/20 sand with octadecyltrichlorosilane according to the method described by Bauters et al. (1998). Two types of sand columns were used. The first type consisted of uniform hydrophobic sand made by mixing in three parts of the strongly hydrophobic sand with 97 parts of regular sand. For the second type the sand columns were filled with regular silica sand except for two 7-cm-thick hydrophobic 12/20 silica sand layers positioned between the 12- to 19- and 31- to 38-cm depths. The hydrophobic layers consisted of a mixture of one part of the strongly water-repellent sand and four parts of regular silica sand. In Exp. II, the columns were wrapped with parafilm to prevent leakage from the water ponded on top of the hydrophobic layer.

In Exp. III, undisturbed 20-cm-diameter soil columns of two soil types with an extensive network of macropores were used: a Hudson silt loam/silty clay loam (firm, moderate coarse prismatic parting to medium, subangular blocky structure) classified as fine, illitic, mesic Glossaquic Hapludalf, and an Arkport sandy loam soil (massive to friable, weak, medium subangular blocky) classified as a coarse-loamy, mixed, mesic Psammentic Hapludalf. The undisturbed soil columns were hand-excavated and then sculpted by hand to a diameter slightly smaller than a 20-cm corrugated culvert pipe. The pipe

was then placed around it and expandable foam (Great Stuff polyurethane) was used to seal the void between the soil and pipe. The Hudson columns were 12 and 20 cm long and the Arkport column was 30 cm long.

Fecal samples were collected from Holstein calves (6–21 d old) exhibiting diagnostic signs of cryptosporidiosis and housed in hutches at the Cornell University Teaching and Research Center in Harford, NY. The samples were obtained by palpating the rectum to induce defecation into sample cups and were then sieved through a food strainer with a 2- to 3-mm mesh to remove large solids and mucus. All collected feces were mixed together, stored in a refrigerator at 4°C until needed, and then mixed again before each use. This procedure ensured uniformity of the input concentration. The oocyst concentration in the fecal samples was determined before the experiments in 100- μ L samples (five replicates) via immunofluorescence staining and microscopic counting (method described below). The oocyst concentration in the mixed fecal sample was 3.5×10^8 oocysts L^{-1} and is representative of that naturally found in calf feces.

In all experiments, distilled water was used as artificial rainfall and applied with a laboratory rainfall simulator slightly modified from Andreini and Steenhuis (1990). The simulator had six needles installed on a frame with rotating patterns in two directions to randomize raindrop distributions. In each experiment, the rain simulator was calibrated using volumetric gauges. In Exp. I, the application rates were 0.3, 1, and 2 $cm\ h^{-1}$. For Exp. II and III, the rainfall intensity was 1 $cm\ h^{-1}$.

Experimental Procedures

In Exp. I and II, two replicate columns were placed simultaneously under the rainfall simulator. One hundred milliliters of feces with 2 g of NaCl salt was applied once on the top surface of all the columns after steady-state flow was reached. At the end of the experiment, using a thin aluminum plate, the soil contained in each ring was carefully separated from the rest of the column and analyzed for both water content and number of oocysts. After the finger flow pattern in each ring was observed and identified, the water content was determined by drying for 24 h at 105°C. Subsamples consisting of porous media and fluid materials were taken within the finger and placed in plastic tubes for microbiological analysis. After the quantity of oocysts was determined, an estimation of the total amount of oocysts in the whole cross section was obtained by multiplying the ratio of the mass of water in the cross section by the mass of water in the subsample by the amount of oocysts in the subsample.

To prevent contamination from previous runs, the rings and funnel were cleaned with chlorine and Ajax (Colgate-Palmolive, New York) commercial solutions using scratch sponges, followed by drying at 105°C for 30 min. Before application of the oocyst–feces mix, effluent samples were analyzed to assess whether oocysts were present.

In Exp. III, 100 mL of feces was mixed with a sufficient amount of KCl to give a concentration of 12.5 $g\ Cl^{-1}\ L^{-1}$ suspension. The mixture was applied on top of soil columns after steady-state flow was reached. Each 50 mL of effluent was sampled, collected in a plastic tube, and analyzed for the number of oocysts and Cl concentration. Soil extractions were only done for the 12-cm-tall column.

Characterization of Preferential Flow Paths

The characterization of preferential flow paths was performed qualitatively in Exp. I and II by adding FD&C blue dye #1 to the infiltrating water, using the same procedure as

in Baveye et al. (1998). After the experiments were finished, blue stains were observed in successive horizontal cross sections. Color photographs of the horizontal cross sections were taken. These pictures were scanned in and the image format was changed from red–green–blue (RGB) to cyan–yellow–magenta–black (CYMK). The cyan channel was retained and converted to black and white images using Adobe Photoshop (Adobe, San Jose, CA).

Chemical and Microbiological Analysis

The Cl^- concentration in the effluent was determined with a digital chloridometer (Buchler Instruments) to obtain the Cl^- breakthrough curves.

The microbiological analysis of *C. parvum* oocysts consisted of immunofluorescence staining to visualize and enumerate oocysts in the samples (Anguish and Ghiorse, 1997). Effluent samples were either directly analyzed or concentrated by centrifugation at 10 000 g for 2 and 15 min for Exp. I and II, respectively. The resulting pellets were resuspended in a fraction of the original liquid and subjected to analysis and counting.

Enumeration of *C. parvum* oocysts in the columns at different depths required a preliminary extraction using the following procedure. About 15- to 20- cm^3 samples of porous medium containing entrapped feces and *C. parvum* were placed in a 50-mL centrifuge tube, to which 15 mL of an extraction solution was added. This solution consisted of 0.1 M phosphate-buffered saline [PBS; 0.028 M $\text{Na}_2\text{HPO}_4 \cdot \text{H}_2\text{O}$, 0.072 M NaH_2PO_4 , 0.145 M NaCl , pH 7.2] and 0.1% by weight of a commercial surfactant, Tween 80 [Polyoxyethylene (20) Sorbitan Monooleate] from J.T. Baker Chemical Co. (Phillipsburg, NJ). The tubes were placed on a horizontal shaker set on low speed (180 rpm) for 20 min and then on the same shaker at high speed (300 rpm) for 10 min. Coarse particles were eliminated in each case by siphoning the slurry into a new centrifuge tube. Fifteen milliliters of a cold sucrose solution (5°C, specific gravity 1.18) was then injected into the centrifuge tubes with a syringe hypodermic needle (18 G 1 1/2) in such a way that the soil–water slurry was on top of, and did not mix with, the sucrose. After centrifugation at 2700 g for 20 min (without automatic braking at the end), the bilayer system in each tube evolved into a trilayer one, with most of the organic matter accumulating into a layer of distinct yellow color. Ten-milliliter aliquots of this intermediate layer were removed using the syringe hypodermic needle, diluted four times with 0.1 M PBS to obtain a total volume of 50 mL, and homogenized by hand. The aliquots were then centrifuged at 2700 g for 30 min (brake on). The bulk (roughly 49 mL) of the supernatant was discarded and the remaining liquid and pellet vortexed on a Fisher (Pittsburgh, PA) vortex genie 2, transferred into a 1.5-mL Eppendorf tube and vortexed again. In each Eppendorf tube, a 100- μL sample was taken for enumeration.

Samples were examined with a Zeiss (Stuttgart, Germany) LSM-210 microscope and observed with an 100X (NA,1.3) oil immersion Neofluar objective lens under both conventional DIC (Differential Interference Contrast) and epifluorescence mode with a triple excitation-emission filter (Chroma Technology Corp., Brattleboro, VT). For optimal imaging, the top element of the 1.4 NA condenser lens was also immersed in oil.

Cryptosporidium parvum oocysts were counted within a smear of a 10- μL sample spread over the slide. The concentration of *C. parvum*, C , in oocysts/L, was calculated as

$$C = (NS)/(FS'V) \quad [1]$$

where N is the number of oocysts counted in F fields, S is the total area covered by the smear (22 by 22 mm for the cover

slide), S' is the area of one of the fields counted with a radius of 0.115 mm, and V is the volume of the smear (10 μL). One hundred fields were counted, giving a standard error of 12.2%.

Mathematical Modeling

Preferential water and solute transport through the profiles has been modeled by assuming that the soil consists of a distribution zone overlaying a conveyance zone (Steenhuis et al., 1994). The distribution zone funnels water and solutes into distinct flow paths of the preferential flow zone. In the transport model for nonadsorbing solutes, the distribution zone acts as a linear reservoir, resulting in an exponential loss of solutes from this zone, and the transport of solutes through the preferential zone is governed by the convective–dispersive equation (Steenhuis et al., 1994; Kim et al., unpublished data, 2003).

The concentration of a nonadsorbing solute in and leaving the distribution zone can be described as (Steenhuis et al., 1994)

$$C = C_0 \exp(-qt/W) \quad [2]$$

where C_0 is the initial concentration, q is the steady-state flow rate, and W is the water content of the distribution zone.

In the conveyance zone, water and solutes flow with an average velocity, v , through the preferential flow paths. If the solute flux in the finger is described with the convective–dispersive equation, the steady-state solution of Eq. [2] at $x = 0$ as a boundary condition and no solutes at the column at $t = 0$ can be found for a conservative solute using Laplace transforms for $4D\lambda/V^2$ (Toride et al., 1995; Kim et al., unpublished data, 2003) as

$$C = \frac{1}{2}C_0 \exp(-\lambda t) \left[\exp\left\{\frac{vx}{2D}(1-\alpha)\right\} \text{erfc}\left(\frac{x-vt\alpha}{2\sqrt{DT}}\right) + \exp\left\{\frac{vx}{2D}(1+\alpha)\right\} \text{erfc}\left(\frac{x+vt\alpha}{2\sqrt{DT}}\right) \right] \quad [3]$$

$$\text{where } \alpha = \sqrt{1 - \frac{4Dq}{Wv^2}}$$

The solution reduces, as expected, to the convective–dispersive solution when $\lambda = 0$ and $C \rightarrow C_0$. The last term can usually be neglected when x or t are sufficiently large; that is, $(x + vt\alpha)/(4Dt)^{1/2} > 3$.

To model the transport of a nonconservative substance like *C. parvum*, a sink term is introduced that describes the removal of *C. parvum* due to adsorbance to the solid–water or AWS interfaces. Assuming that the removal is irreversible and proportional to the concentration in solution, the loss of *C. parvum* from the distribution zone becomes

$$C = C_0 \exp\left[-\left(\frac{q}{W} + \beta\right)t\right] \quad [4]$$

where β is the first-order rate of removal from the solution. The concentration in the conveyance zone can be described for $(x + vt\alpha)/(4Dt)^{1/2} > 3$ as

$$C = \frac{1}{2}C_0 \exp\left[-\left(\frac{q}{W} + \beta\right)t\right] \left\{ \exp\left[\frac{vx}{2D}(1-\alpha')\right] \text{erfc}\left(\frac{x-vt\alpha'}{\sqrt{4Dt}}\right) \right\} \quad [5]$$

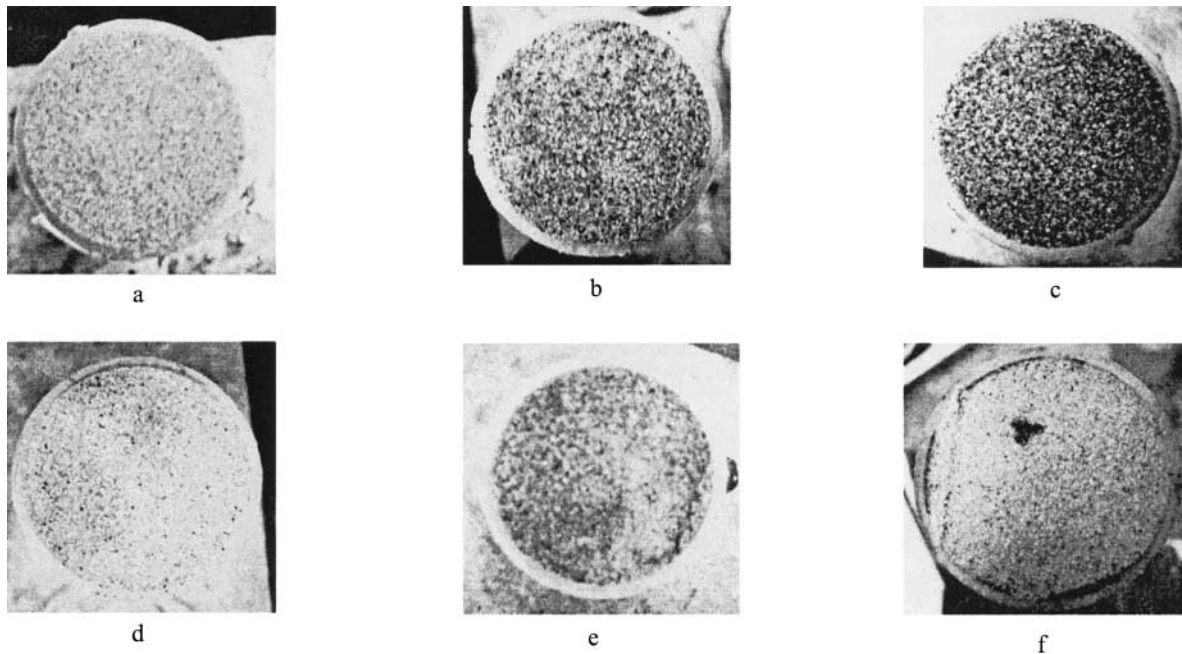


Fig. 2. Examples of blue dye distribution for various locations in the columns and at different flow rates: (a) the distribution zone, (b) immediately above the capillary fringes, and (c) in the capillary fringes. The number of fingers formed was different for the various flow rates: (d) 1 cm h⁻¹ in Exp. I, (e) 2 cm h⁻¹ in Exp. I, and (f) for the column with hydrophobic sand in Exp. II.

$$\text{where } \alpha' = \sqrt{1 - \frac{4D\left(\frac{q}{W} + \beta\right)}{v^2}}$$

RESULTS

Fingered Flow Experiments

Analysis of Dye Patterns

The flow pattern through the soil profile in the sand columns of Exp. I and II is discussed first. In the top and bottom portions of the sand columns, the FD&C blue dye was nearly uniformly distributed as shown for the distribution zone in Fig. 2a, and immediately above and in the capillary fringes in Fig. 2b and 2c, respectively. There was also a capillary fringe above the water-repellent layers (not shown). In the intermediate, unsaturated conveyance zone, fingers occurred. The lateral boundaries of these fingers were somewhat diffuse, making a quantitative analysis of their relative area at various depths somewhat subjective. The number of fingers depended on the flow rate and medium. At the lower rainfall rate in the regular sand, there were fewer fully formed fingers (Fig. 2d) than at the high rainfall rate, where the fingers were markedly more diffuse and occupied a higher proportion of the cross-sectional area (Fig. 2e). Hydrophobicity of the sand increased the instability of water flow in the columns, and one small, narrower finger was observed as a result in the water-repellent layers (Fig. 2f). Previous blue staining experiments (Steenhuis et al., 1994) showed that there is an extensive network of macropores in the Hudson soil. Both matrix and macropore flow occurred in the Arkport soil.

Concentration of Chloride and *Cryptosporidium parvum* Oocysts in Drainage Water

In all cases, the replicate columns gave similar Cl⁻ breakthrough curves for the sand columns in Exp. I and II (Fig. 3). For these sand columns, there was a direct relationship between the application rate and the amount of water required for initial breakthrough of the Cl⁻. For the low application rate of 0.3 cm h⁻¹, breakthrough was almost immediately, whereas for the 2 cm h⁻¹ case, significant breakthrough only occurred after application of 1.6 cm of drainage water. These differences were expected since the velocity of the fingers depends only on the soil properties—the wetted area adjusts itself to the applied flux. So, for a high application rate, more fingers carry the flow than for a low application rate (Fig. 2d and 2e confirm this). Consequently, more water was required for a larger wetted area for the high application rate than for the low flow rate where the area wetted was smaller.

Although for the sand columns in Exp. I and II more variation in the *C. parvum* oocysts concentration existed in the drainage water than for the Cl⁻, some similarities were apparent (Fig. 3). Besides that the replicates were extremely close, the *C. parvum* oocysts breakthrough occurred at the same time as the Cl⁻. The oocysts peak also occurred at approximately the same time or sometimes slightly before the Cl⁻ peak. The decrease in oocysts concentrations below the detection limit was almost as fast as the rise to the peak concentration, so that the oocysts concentrations reached zero after only 1.5 to 3 cm of drainage effluent (100–200 min after the rain started). This was markedly different than the long tail of the Cl⁻ concentration.

Figure 4 displays the moisture content, as well as the

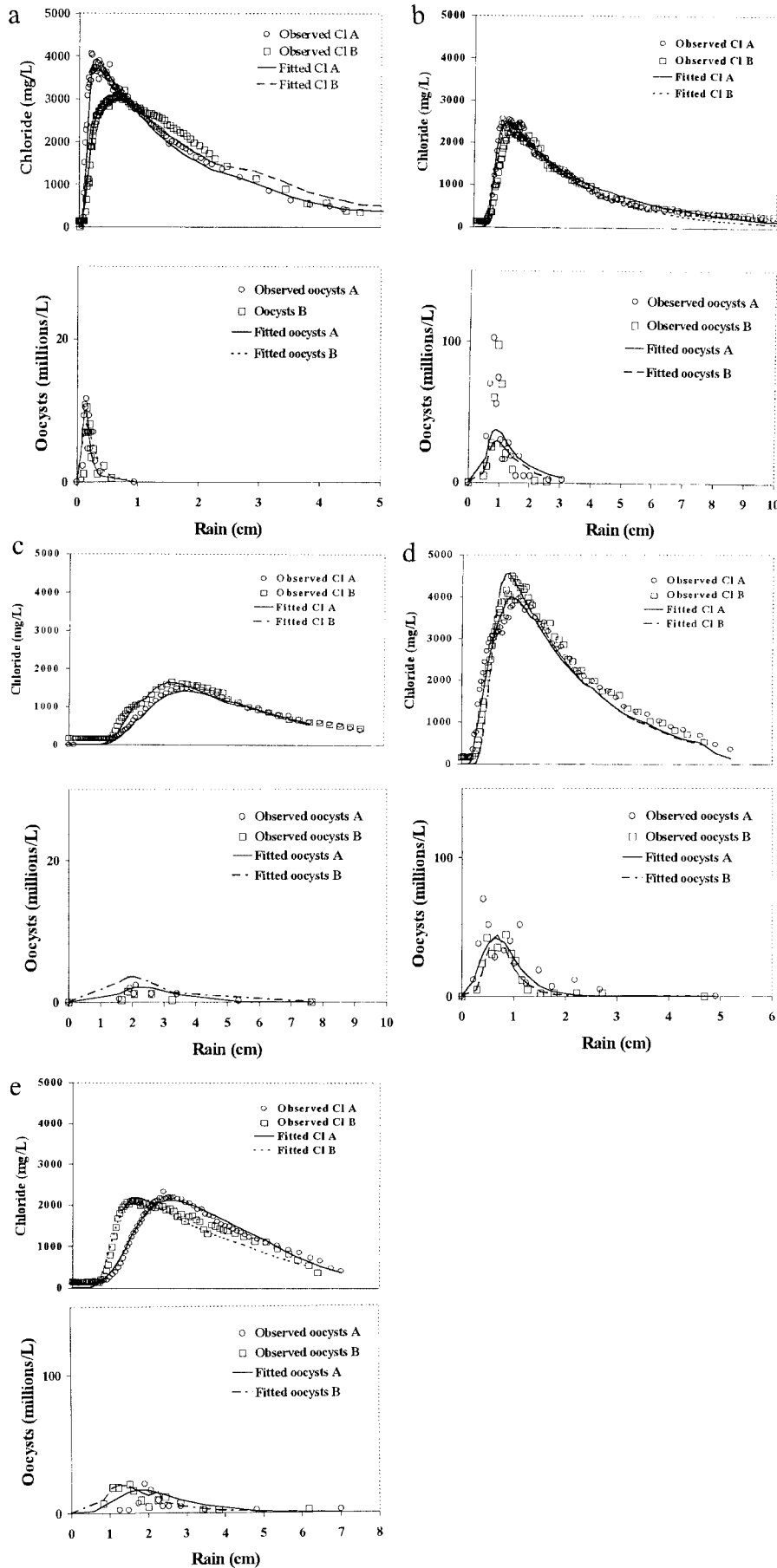


Fig. 3. Breakthrough curves and model prediction of Cl⁻ and *C. parvum* oocysts in regular and water-repellent 12/20 silica sand. Initial concentrations in the applied feces was 12.5 g Cl⁻ L⁻¹ and 3.5 × 10⁸ *C. parvum* oocysts L⁻¹, (a) 0.3 cm h⁻¹ rainfall (regular sand, Exp. I), (b) 1 cm h⁻¹ rainfall (regular sand, Exp. I), (c) 2 cm h⁻¹ rainfall (regular sand, Exp. I), (d) 1 cm h⁻¹ rainfall (water-repellent sand, Exp. II), and (e) 1 cm h⁻¹ rainfall (regular sand with two water-repellent layers, Exp. II).

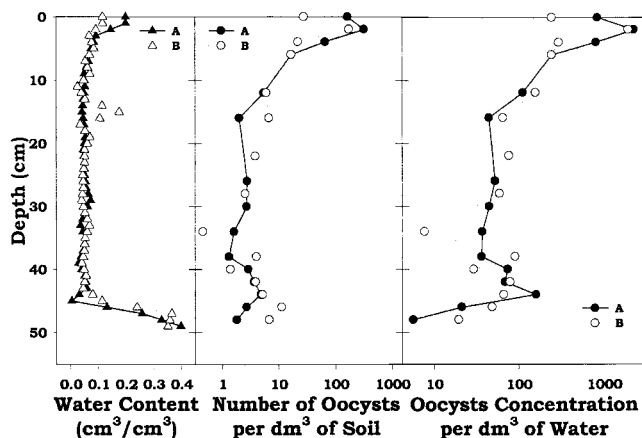


Fig. 4. Water saturation profile and spatial distribution of *C. parvum* oocysts in 12/20 silica sand resulting from a 2 cm h^{-1} rainfall event (Exp. I).

concentration and mass of *C. parvum* oocysts retained in the sand columns. The moisture content (as percentage of saturation) was again similar for all of the sand columns. Moisture contents were elevated in the top 3 to 5 cm where the distribution zone was located and near the bottom of the column in the capillary fringe. In addition, the moisture contents were greater in the capillary fringes above both water-repellent layers in Exp. II. In the conveyance zone, the average water content was low. As expected, the average water content increased for the increasing flow rates within Exp. I because a larger portion of the columns was wetted, resulting in a higher average moisture content. Since the water contents were taken after the water application was stopped, some drainage took place before the samples were taken and, consequently, the moisture contents in the distribution and conveyance zones are underestimated.

For all sand columns, the *C. parvum* concentration was the greatest in the distribution zone near the surface. This is exemplified by the two replicate columns of Exp. I with the 2 cm h^{-1} flow rate (Fig. 4). The *C. parvum* oocysts concentration in the conveyance zone was more or less constant, with some tendency to be slightly higher in the capillary fringes, but this was not consistent. Consequently, the highest oocyst quantities were found at the surface and within a region immediately above the capillary fringe at the same location where the average moisture contents in the columns were relatively the greatest.

If we compare the breakthrough curves for Exp. III (Fig. 5) and Exp. I and II (Fig. 3), it took a longer time for the Cl^- to initially appear but the overall shape of the breakthrough curves was approximately the same. The differences in *C. parvum* oocysts were more significant. In the Hudson column, application of the manure at the soil surface resulted in a rapid decrease of the water outflow rate (Fig. 6). After about 3 cm of rain, this decrease stopped and the outflow rate began to increase. By the end of the experiment, it had returned to 75% of its original value (Fig. 6). The time where the outflow of the column started to increase coincided

with the appearance of oocysts in the effluent (Fig. 5b), significantly later than the peak in Cl^- concentration. In the Arkport soil column (Fig. 5c), oocysts appeared in the effluent during the tailing of the Cl^- breakthrough curve. Thereafter, the oocyst breakthrough had an erratic pattern and continued after the Cl^- concentration had subsided.

The simultaneous first appearance of *C. parvum* oocysts and Cl^- in the drainage water of the sand columns indicated that there was no retardation in the movement of *C. parvum* oocysts compared with Cl^- and that apparent reversible adsorption in the classical sense did not occur. Classical reversible adsorption would have produced a delay in the *C. parvum* concentration such as observed in Exp. III. In both cases, the mass recovered was much less than applied, indicating that there was a nonreversible reaction during the time frame of the experiments, which took the oocysts out of the solution.

Mass Balance

Despite the fact that recovery of *C. parvum* oocysts in soils was uncertain (Mawdsley et al., 1996; McElroy et al., 2001), the numbers of oocysts in the columns were measured after the columns were taken apart. By adding the quantity in the column with what was lost in the drainage water and comparing with the amount originally added, the percentage recovered could be calculated (Table 1). The wide range of recoveries from 14 to 86% is the same as reported in the literature (Brush et al., 1999). This variability might have been caused by any one of the various steps involved in the cumbersome procedure used for the enumeration of the oocysts. In addition, variability may be caused by the necessity of taking subsamples. Particularly in the distribution zone where fingers develop, this sampling may have introduced artifacts that were, unfortunately, impossible to avoid at this stage, for lack of a better enumeration technique.

Mathematical Modeling

To investigate how well Eq. [5] can predict the breakthrough of *C. parvum* oocysts, we first obtained the values for the water content of the distribution layer, the velocity and the dispersion coefficients for the conveyance zone using the Cl^- breakthrough curves. Then these values were used for finding the first-order degradation constant, β , by fitting Eq. [5] to the observed *C. parvum* oocysts breakthrough curves. If the β values were internally consistent and agreed with literature values, the equation could be considered valid. The best fit values of the distribution water content, W , velocity, v , and dispersion coefficient in the conveyance zone for the sand column Cl^- breakthrough data are shown in Table 2. The values for the sand columns were internally consistent. The water contents in the distribution zone between 1.8 and 3.4 cm were in the range that is in agreement with the moisture contents in Fig. 5.

The velocities for the sand column for Exp. I were also remarkably constant around 36 cm h^{-1} with the exception of the higher velocity of 60 cm h^{-1} in replicate

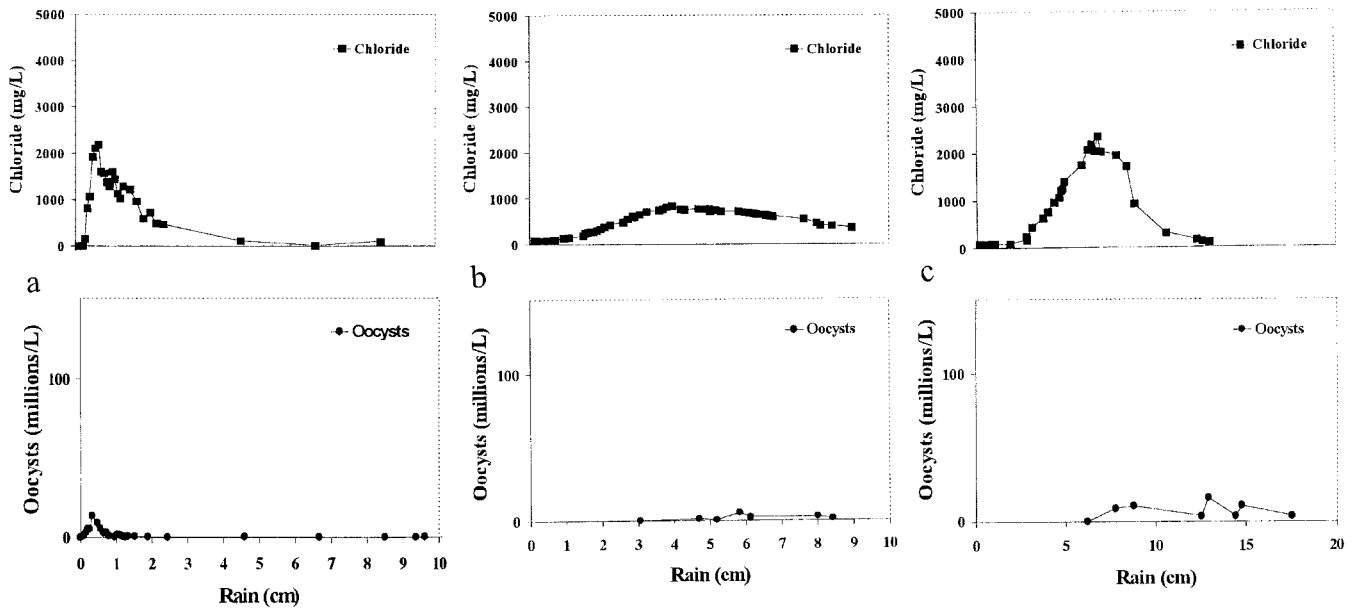


Fig. 5. Breakthrough curves and model prediction of Cl^- and *C. parvum* oocysts in undisturbed soil columns for Exp. III. Initial concentrations in the applied feces was $12.5 \text{ g Cl}^- \text{ L}^{-1}$ and $3.5 \times 10^8 \text{ C. Parvum oocysts L}^{-1}$. (a) 12-cm Hudson soil column, (b) 20-cm Hudson soil column, and (c) 30-cm Arkport soil column.

A of the experiment with an 1 cm h^{-1} rainfall, and of the lower velocity of 18 cm h^{-1} in replicate B with a 0.3 cm hr^{-1} rainfall. The variation for two exceptions was not significant compared with the velocities obtained for water-repellent sands, as we see later. As discussed above, this was a direct result of the finger velocities being independent of the flow rate and dependent on the media properties. In fact, the values are in line with what would be expected for this type of sand, such as a saturated moisture content of $0.37 \text{ cm}^3 \text{ cm}^{-3}$. In Exp. II, the velocities for the water-repellent sand columns were almost two to six times higher than in other sand column experiments with lower W values than in the 1 cm h^{-1} regular sand experiments, while the two layer columns did not show a significant difference in values. It was not surprising to obtain high velocities for water-repellent columns (Table 2), and the wetted area was much smaller (Fig. 2f) as this water repellency shortened the travel time (Bauters et al., 1998).

Dispersivities for all sand columns were in the reasonable range of 1.0 to 6.7 cm. The model predicts Cl^- breakthrough curves well, with high R^2 values of >0.97 for all columns. Using these parameters, we estimated a β (Eq. [4]) that would best fit the oocysts concentrations.

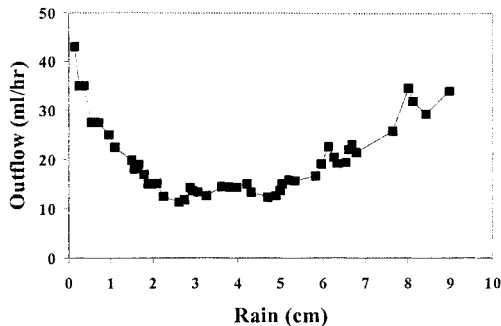


Fig. 6. Soil column flow rate from 20-cm Hudson soil column A.

The β values found ranged from 0.6 to 1.8 h^{-1} and were higher than literature values of 0.004 and 0.09 h^{-1} for the medium and fine sand, respectively, by Wan and Tokunaga (1997), and 0.1 h^{-1} for experiments of saturated porous media with *E. coli*. by Stevik et al. (1999). The higher β values in this study were a result of a higher retention of *C. parvum* in the unsaturated columns compared with the saturated columns.

Illustrations of the fit are shown in Fig. 3. The model did not fit the oocyst breakthrough curves as well as the Cl^- curves, but was overall predictable with R^2 values of >0.70 , although some exceptions occurred. The largest discrepancy was observed for a 1 cm h^{-1} rainfall experiment, in which only one-half the observed oocysts were predicted. The better fitting results for the other two rainfall intensity columns in Exp. I using the same parameters obtained from the Cl^- breakthrough curves suggest that the observed oocyst data were overestimated by the technical error. For all columns, peaks occurred at the same time for *C. parvum* and Cl^- , but *C. parvum* showed a much faster decrease in concentration.

Table 1. Total recovery of *C. parvum* oocysts in experiments with 12/20 silica sand columns, inferred from oocyst counts in the effluents and from their spatial distribution inside the sand columns.

Exp.	Soil type	Column	Oocysts			Recovery %
			BTC	Profile	Total	
I	Sand 0.3 cm h^{-1}	A	2.97	94.9	97.9	28
		B	3.15	46.1	49.2	14.1
	Sand 1 cm h^{-1}	A	104	1.49	253	73.4
		B	71.1	53.9	124	35.8
	Sand 2 cm h^{-1}	A	5.38	185	190	54.4
		B	2.09	105	107	30.6
II	Water repellent	A	81.4	201	282	80.8
		B	47.3	254	301	86.2
	Two layers	A	43.4	93.2	136	39
		B	67.1	165	232	66.4

Table 2. Parameters used for fitting the model to the experimental results: q , flow rate; W , apparent water content; v , pore water velocity; D , dispersion coefficient; ϕ , dispersivity (d/v); β , rate of removal from the solution; R^2 , correlation coefficients.

Exp.	Soil type	Column	q	W	v	D	ϕ	β	R^2	
									Cl^-	Oocysts
I	Sand 0.3 cm h^{-1}	A	0.3	1.8	30	60	2	1.2	1	0.7
		B		2	18	120	6.7	1.2	1	0.7
	Sand 1 cm h^{-1}	A	1	2.8	60	60	1	0.6	1	0.5
		B		2.5	42	54	1.3	0.6	1	0.61
	Sand 2 cm h^{-1}	A	2	3.4	30	60	2	1.8	1	0.74
		B		3.2	36	60	1.7	1.8	1	0.72
II	Water repellent	A	1	1.6	102	300	2.9	0.6	1	0.6
		B		1.5	108	120	1.1	1.8	1	0.85
	Two layers	A	1	2	24	120	5	0.6	1	0.49
		B		2.8	36	48	1.3	0.6	1	0.79

One exception is replicate A of the experiment with two water-repellent interfaces in Exp. II, in which an oocyst increase was delayed a little compared with the Cl^- breakthrough. This resulted in a low R^2 value for modeling this column.

DISCUSSION

The experimental results presented in Fig. 3 and 5 clearly show the ability of preferential flow—fingering and macropore—to transport large numbers of oocysts through the relatively short unsaturated columns. In all fingering flow experiments, the number of oocysts found in the effluents are orders of magnitude greater than needed to cause cryptosporidiosis in healthy adults. However, under field conditions, there is usually a longer path through the vadose zone and the concentration will be less.

The results shown in Fig. 5 suggest that in clay soils, oocyst breakthrough may be limited compared with that in other soils, in spite of the presence of macropores. However, the drastic reduction of outflow rate immediately after addition of the feces indicated that some of the macropores became severely clogged with the feces material. Unclogging of the macropores and resumption of flow permitted the passage of oocysts in large numbers shortly thereafter.

Despite the uncertainty of the initial oocyst number applied, it is clear that the oocyst numbers predicted through 50-cm sand columns were reduced by two orders of magnitude from hundreds of millions to several millions. Therefore, if the rain water has to percolate through several meters of soil before reaching the groundwater, contamination risks should be minimal. However, in the cases where the groundwater is shallow and the source of the *C. parvum* oocysts and the drinking water well are close together, contamination of well water with *C. parvum* oocysts could occur on a sandy soil after a rainstorm. A realistic example could be a sick animal defecating near a well during a county fair with temporary shallow wells on a sandy flood plain soil.

It is of interest to compare our results of breakthrough experiments of *C. parvum* oocysts in unsaturated columns with those performed by Brush et al. (1999) and Harter et al. (2000), where the columns were saturated. Comparing the two flow regimes, the main difference is that under unsaturated conditions, the *C. parvum*

oocysts concentration in the effluent decreases faster than the Cl^- , while for the saturated columns there was a significant tailing in the latter part of the breakthrough curve and a measurable concentration was observed throughout the duration of the experiment (Harter et al., 2000). Therefore, to simulate the breakthrough of *C. parvum* oocysts, Harter et al. (2000) had to assume that the attachment of the oocysts to grains was reversible, while for unsaturated conditions we assumed that the attachment was irreversible. The latter is consistent with the results of Crist et al. (2003) who recorded the pore-scale distribution of colloids in still and video images. They found that the hydrophilic, negatively charged carboxylated latex microspheres, which have similar characteristics as *C. parvum* oocysts, were retained primarily in a thin film of water at the edge of the menisci at the AWS interface. Under steady-state flow conditions (as was the case in our experiments), the microspheres stayed in place and did not go back into the solution. Under saturated conditions, meniscus (and the AWS interfaces) do not exist, and other mechanisms of retention become important such as filtration in narrow pore spaces. Retention by filtration is likely less permanent and allows remobilization. Consequently, it is not unexpected that the modeling retention of *C. parvum* oocysts under saturated and unsaturated conditions is different.

Finally, it is of interest to note that the flow rate was independent of the time it took for the *C. parvum* oocysts to reach the bottom of the columns in Exp. I (i.e., velocity and flow rate are not related in Table 2). Since the velocity of the fingers only depends on the type of porous media, mass balance consideration dictates that more fingers form under increasing flow rates in initially dry sand (Steenhuis et al., 2001). Thus, the likelihood of pollution of aquifers depends partly on the duration of the rainstorm.

CONCLUSIONS

The results of laboratory breakthrough experiments suggest that significant numbers of *C. parvum* oocysts are able to percolate through 50-cm-long sand and soil columns under conditions where preferential flow occurs. The transport of oocysts was modeled based on a partitioning of the soil profile in both a distribution and conveyance zone with preferential flow and by assuming

irreversible retention at the AWS interfaces. The model was able to simulate the markedly asymmetric breakthrough patterns for *C. parvum* oocysts in sand columns with preferential fingered flow. The retention mechanisms of *C. parvum* oocysts is significantly different under saturated and unsaturated conditions.

ACKNOWLEDGMENTS

This research was sponsored by the National Research Initiative, United States Department of Agriculture, under grant/contract 96-35102-3839. The Reviewers contributed significantly to a more readable manuscript.

REFERENCES

- Andreini, M.S., and T.S. Steenhuis. 1990. Preferential paths of flow under conventional and conservational tillage. *Geoderma* 46:85–102.
- Anguish, L.J., and W.C. Ghiorse. 1997. Computer-assisted laser scanning and video microscopy for analysis of *Cryptosporidium parvum* oocysts in soil, sediment and feces. *Appl. Environ. Microbiol.* 63:724–733.
- Atwill, E.R., R.A. Sweitzer, M.D.C. Pereira, I.A. Gardner, D. van Vuren, and W.M. Boyce. 1997. Prevalence of and associated risk factors for shedding *Cryptosporidium parvum* oocysts and *Giardia* cysts within fecal pig populations in California. *Appl. Environ. Microbiol.* 63:3946–3949.
- Bauters, T.W.J., D.A. DiCarlo, T.S. Steenhuis, and J.-Y. Parlange. 1998. Preferential flow in water repellent sands. *Soil Sci. Soc. Am. J.* 62:1185–1190.
- Baveye, P., C.W. Boast, S. Ogawa, J.-Y. Parlange, and T.S. Steenhuis. 1998. Influence of image resolution and thresholding on the apparent mass fractal characteristics of preferential flow patterns in field soils. *Water Resour. Res.* 34:2783–2796.
- Brush, C.F., W.C. Ghiorse, L.J. Anguish, J.-Y. Parlange, and H.G. Grimes. 1999. Transport of *Cryptosporidium parvum* oocysts through saturated columns. *J. Environ. Qual.* 28:809–815.
- Craun, G.F., S.A. Hubbs, F. Frost, R.L. Calderon, and S.H. Via. 1998. Waterborne outbreaks of cryptosporidiosis. *J. Am. Water Works Assoc.* 90:81–91.
- Crist, J.T., J.F. McCarthy, Y. Zevi, P.C. Baveye, J.A. Throop, and T.S. Steenhuis. 2003. Pore-scale visualization of colloid transport and retention in partly saturated porous media. *Vadose Zone J.* (in press).
- Current, W.L. 1986. *Cryptosporidium*: Its biology and potential for environmental transmission. *Crit. Rev. Environ. Control* 17:21–51.
- Galbraith, N.S., N.J. Barrett, and R. Stanwell-Smith. 1987. Water and disease after Croydon: A review of waterborne and water-associated disease in the U.K. 1937–1986. *J. Inst. Water Environ. Man.* 1:7–21.
- Harter, T., S. Wagner, and E.R. Atwill. 2000. Colloid transport and filtration of *Cryptosporidium parvum* in sandy soils and aquifer sediments. *Environ. Sci. Technol.* 34:62–70.
- Hayes, E.B., T.D. Matte, T.R. O'Brian, T.W. McKinley, G.S. Logsdon, J.B. Rose, B.L.P. Ungar, D.M. Word, P.F. Pinsky, M.L. Cummings, M.A. Wilson, E.G. Long, E.S. Hurwitz, and D.D. Juraneck. 1989. Contamination of a conventionally treated filtered public water supply by *Cryptosporidium* associated with a large community outbreak of cryptosporidiosis. *N. Engl. J. Med.* 320:1372–1376.
- MacKenzie, W.R., N.J. Hoxie, M.E. Procter, M.S. Gradus, K.A. Blair, D.E. Peterson, J.J. Kazmierczak, D.G. Addiss, K.R. Fox, J.B. Rose, and J.P. Davis. 1994. A massive outbreak in Milwaukee of *Cryptosporidium* infection transmitted through the public water supply. *N. Engl. J. Med.* 331:161–167.
- Mawdsley, J.L., A.E. Brooks, and R.J. Merry. 1996. Movement of the protozoan pathogen *Cryptosporidium parvum* in three contrasting soil types. *Biol. Fertil. Soils* 21:30–36.
- McElroy, W., E. Cabello, and S.D. Pillai. 2001. Efficacy of an immunomagnetic separation system for recovering *Cryptosporidium* oocysts from soils. *J. Rapid Meth. Automat. Microbiol.* 9:63–70.
- Rose, J.B., C.P. Gerba, and W. Jakubowski. 1991. Survey of potable water supplies for *Cryptosporidium* and *Giardia*. *Environ. Sci. Technol.* 25:1393–1400.
- Smith, H.V., R.W. A. Girdwood, W.J. Patterson, R. Hardie, L.A. Green, C. Benton, W. Tulloch, J.C.M. Sharp, and G.I. Forbes. 1988. Waterborne outbreak of cryptosporidiosis. *Lancet* 1484:8626–8627.
- Smith, H.V. 1992. *Cryptosporidium* and water: A review. *J. Inst. Water Environ. Manage.* 6:443–451.
- Steenhuis, T.S., J. Boll, G. Shalit, J.S. Selker, and I.A. Merwin. 1994. A simple equation for predicting preferential flow solute concentrations. *J. Environ. Qual.* 23:1058–1064.
- Steenhuis, T.S., Y.-J. Kim, J.-Y. Parlange, M.S. Akhtar, B.K. Richards, K.-J.S. Kung, T.J. Gish, L.W. Dekker, C.J. Ritsema, and S.A. Aburime. 2001. An equation for describing solute transport in field soils with preferential flow paths. p. 137–140. *In* D.D. Bosch and K.W. King (ed.) *Preferential flow, water movement and chemical transport in the environment*. Proc. ASAE 2nd Int. Symp. Honolulu, HI. 3–5 Jan. 2001.
- Stevik, T.K., G. Ausland, J.F. Hanssen, and P.D. Jenssen. 1999. The influence of physical and chemical factors on the transport of *E. coli* through biological filters for wastewater purification. *Water Res.* 33:3701–3706.
- Toride, N., F. Leij, and M.Th. van Genuchten. 1995. The CXTFIT code for estimating transport parameters from laboratory or field tracer experiments. Version 2.2. Res. Rep. 137. U.S. Salinity Lab., Riverside, CA.
- Wan, J., and T.K. Tokunaga. 1997. Film straining of colloids in unsaturated porous media: Conceptual model and experimental testing. *Environ. Sci. Technol.* 31:2413–2420.